NASA Contractor Report 4001

Wave Propagation in Anisotropic Medium Due to an Oscillatory Point Source With Application to Unidirectional Composites

James H. Williams, Jr., Elizabeth R. C. Marques, and Samson S. Lee

GRANT NAG3-328
JULY 1986

NASA

NASA Contractor Report 4001

Wave Propagation in Anisotropic Medium Due to an Oscillatory Point Source With Application to Unidirectional Composites

James H. Williams, Jr., Elizabeth R. C. Marques, and Samson S. Lee

Massachusetts Institute of Technology
Cambridge, Massachusetts

Prepared for
Lewis Research Center
under Grant NAG3-328

National Aeronautics
and Space Administration

Scientific and Technical Information Branch

1986

INTRODUCTION

The expanding uses of composite materials, especially of the filamentary type, require the generation of a variety of data on material behavior so that adequate design can be achieved. Many test techniques have been developed for such purposes. Among these are the nondestructive evaluation (NDE) techniques of ultrasonics and acoustic emission.

The application and interpretation of results obtained from various NDE techniques are strongly related to the stress wave propagation characteristics of the material. The theoretical prediction of the stress wave fields under the action of well defined excitation can give information regarding the proper use of the NDE techniques, and may provide improved precision of a material's diagnosis by establishing more quantitative standards.

Via an asymptotic approximation, the stress wave field generated by a point source in an infinite anisotropic medium can be described in analogy with the problem of magnetohydrodynamic waves discussed by Lighthill [1]. For the present work, the particular case of transversely isotropic media is presented by following the same procedure used by Buchwald [2], where here the solution is extended such that the displacements are obtained and expressed in cartesian form.

Here, the solution is given for the case of a glass fiber

reinforced epoxy unidirectional composite. The slowness and wave surfaces are determined as well as the displacements for points throughout the medium. Polar diagrams for displacement amplitudes are constructed illustrating the patterns of the displacement field.

Other aspects of the problem of stress waves in homogeneous anisotropic media can be found in the studies of Synge [3], Carrier [4] and Musgrave [5]. Synge analyzed the behavior of stress waves in a single layer of anisotropic material subjected to uniform stress at one of its surfaces and extended the study to the limiting case where the layer is transformed into a half space. Carrier proposed a solution for waves in an infinite medium using potential functions and integral techniques. Musgrave established the conditions to be satisfied for the existence of the general equation of motion when a plane wave solution is adopted and described the geometry of the spreading disturbances by means of the wave surfaces and slowness surfaces.

The work on layered media was carefully explored but was not pursued for this research. The primary reason for this is that general anisotropy is a more convenient approach for representing a composite because the effective modulus theory can be used to model the material as homogeneous [6]. It is assumed that the material behaves as homogeneous since the layer thicknesses (fiber diameter for filamentary composites) are small as compared with the wavelengths. If this requirement is satisfied, the effective

modulus theory appears to describe the behavior of stress waves in laminated composites better than the laminated media theory [7,8].

EQUATION OF MOTION AND ITS SOLUTION

A schematic of the system under investigation is shown in Fig. 1. An infinite transversely isotropic medium is subjected to a point force source which generates stress waves that propagate throughout the medium. A cartesian coordinate system x, y and z is adopted such that the x-y plane is the isotropic plane in the medium. In a unidirectional composite, z would be the fiber direction. The point source is located at the origin and oscillates in the x direction as shown. The displacements at any point P in the medium due to a steady-state sinusoidal point force excitation are analyzed.

Force-Dynamic Equations

The force-dynamic equations for an infinite medium can be derived from the equilibrium conditions of a differential volumetric element and are given as [9]

$$\rho u_{j,tt} = \tau_{ij,i} + \rho F_j \qquad (1)$$

where the implied summation is over the repeated subscripts, ρ is the mass density, the indices i and j have values x, y and z in a rectangular cartesian coordinate system, u_j is the displacement in the j direction, τ_{ij} is the stress tensor and F_j is the body force (force per unit mass) in the j direction. The indices following the comma

refer to partial derivatives such that $u_{j,tt}$ represents the second derivative of the jth component of displacement with respect to t, the time variable.

For the point sinusoidal force shown in Fig. 1, the body forces can be written in exponential form as

$$F_x = F_o\, \delta(x)\delta(y)\delta(z)\, e^{-i\omega t} \qquad \text{and} \qquad F_y = F_z = 0 \tag{2}$$

where $i = (-1)$, ω is the radian frequency of the harmonic excitation, $\delta(\ )$ is the Dirac delta function and F_o is the force amplitude. The actual oscillatory force is taken as the real part of the expression for F_x in eqn. (2).

Constitutive Relations

The constitutive relations based on Hooke's law are [10]

$$\tau_{ij} = C_{ijpq}\, \varepsilon_{pq} \tag{3}$$

where C_{ijpq} are the elastic coefficients that constitute the stiffness matrix and ε_{pq} is the strain tensor that can expressed in terms of displacements using the engineering definitions for strains as

$$\varepsilon pq = \frac{1}{2}(u_{p,q} + u_{q,p}) \tag{4}$$

where the suffixes each represent the x, y and z directions. The

elastic coefficients satisfy the symmetry conditions such that [11]

$$C_{ijpq} = C_{jipq} = C_{ijqp} = C_{pqij} \tag{5}$$

The four indices notation for the elastic coefficients can be modified to the two indices compact form [9]. In this case, the stress tensor is written as a vector

$$\tau_1 = [\tau_1, \tau_2, \tau_3, \tau_4, \tau_5, \tau_6] \tag{6}$$

where the equivalence in the cartesian system is $\tau_1 = \tau_{xx}$, $\tau_2 = \tau_{yy}$, $\tau_3 = \tau_{zz}$, $\tau_4 = \tau_{xz}$, $\tau_5 = \tau_{yz}$, $\tau_6 = \tau_{xy}$. The same correspondence is applicable for the strains.

For a transversely isotropic medium as shown in Fig. 1, where the x - y plane is the isotropic plane, z is the symmetry axis of the medium. It can be shown that for transversely isotropic materials, there are five independent elastic coefficients [11]. The nonzero elastic coefficients according to the definition of the stress components in eqn. (6) are

$$C_{11} = C_{22},\ C_{33},\ C_{12},\ C_{13} = C_{23},\ C_{44} = C_{55} \text{ and } C_{66} = \frac{1}{2}(C_{11} - C_{12}) \tag{7}$$

Constraints

The constraints are introduced by the application of the "radiation condition". Since the medium is infinite, the constraint

is that no waves originate at infinity or are reflected at infinity; that is, the only source of disturbance is due to the point force located at the origin of the coordinate system. From this assumption, the amplitudes of the displacements must decrease with distance from the source. In the limit, as the distance approaches infinity, the displacement amplitudes must vanish.

Equations of Motion

The equations of motion can be represented in terms of the displacements by substituting eqns. (4) and (5) into eqn. (3) and then substituting the result into eqn. (1) to give [10]

$$\rho u_{j,tt} = C_{ijpq}\, u_{p,qi} + \rho\, F_j \qquad (8)$$

where the symmetry condition given in eqn. (5) is utilized. The forcing function is as given in eqn. (2). For a transversely isotropic medium, the elastic coefficients obey eqn. (7).

Solution of Equations of Motion

The equations of motion are given in eqn. (8) and must be solved in accordance with the imposed constraints and the applied forces described earlier.

Eqn. (8) can be rewritten using u, v and w for the displacements in the x, y and z directions, respectively, instead of u_x, u_y and u_z; and using x, y and z for the subscripts denoting

derivatives. This gives three equations in u, v and w. Then these equations can be differentiated with respect to the space and time variables to give terms in $u_{,ttx}$, $u_{,tty}$, $v_{,ttx}$, $v_{,tty}$ and $w_{,ttz}$ which can be combined by addition and subtraction to give [2]

$$\Lambda_{,tt} = a_4 \nabla_1^2 \Lambda + a_5 \Lambda_{,zz} + F_{x,y} \tag{9}$$

$$\Gamma_{,tt} = a_3 \Delta_{,zz} + a_5 \Delta_1^2 \Gamma + a_2 \Gamma_{,zz} \tag{10}$$

$$\Delta_{,tt} = a_3 \nabla_1^2 \Gamma + a_5 \Delta_{,zz} + a_1 \nabla_1^2 \Delta + F_{x,x} \tag{11}$$

where the new variables are

$$\begin{aligned} \Lambda &= v_{,x} - u_{,y} \\ \Gamma &= w_{,z} \\ \Delta &= u_{,x} + v_{,y} \end{aligned} \tag{12}$$

Λ represents the z component of rotation, Γ is the strain in the z direction and $(\Gamma + \Delta)$ is the dilatation, all in accordance with standard definitions in elasticity. Physically, the fact that a separate equation for the z rotation can be written, namely eqn. (9), indicates that the propagation of these rotational waves is independent of the other possible modes. The same is not true for the displacement functions Γ and Δ, since eqns. (10) and (11) cannot be decoupled. The a's are constants given by

$$a_1 = \frac{C_{11}}{\rho} \ , \quad a_2 = \frac{C_{33}}{\rho} \ , \quad a_3 = \frac{C_{44}+C_{13}}{\rho} \ , \quad a_4 = \frac{C_{11}-C_{12}}{2\rho} \ , \quad a_5 = \frac{C_{44}}{\rho} \tag{13}$$

and ∇_1^2 is the laplacian operator in two dimensions such that

$$\nabla_1^2 = \frac{\partial^2}{\partial x^2} + \frac{\partial^2}{\partial y^2} \tag{14}$$

If eqn. (2) is substituted into eqns. (9), (10) and (11), the asymptotic solution can be obtained by using Fourier integrals and the method of stationary phase [12]. Basically, eqns. (9), (10) and (11) are written in terms of Fourier integrals. In doing this, plane wave solutions are assumed with associated wave number vectors that are represented by their components α along the x direction, β along the y direction and γ along the z direction. Then, the values of the Fourier integrals are approximated by their residues such that the stationary points are determined by the singularities of the integrands. In this approximation, terms involving the factor $1/r^2$ (where r is the radial distance from the origin to P the point of interest) are neglected. Thus, the expressions obtained are adequate for the calculation of the displacements of points in the thus defined far field. This leads to the following results [2]

$$\Lambda \tilde{=} \frac{i \beta F_o}{2\pi r |\underline{\nabla G}| (|K_G|)^{1/2}} \exp [i(\alpha x + \beta y + \gamma z - \omega t)] \tag{15}$$

$$\Delta \simeq \frac{1}{2\pi r} \sum_{n=1}^{N} \frac{A_n \, i \, F_o}{|\underline{\nabla H}|\,(|K_H|)^{1/2}} \alpha_n [a_5(\alpha_n^2+\beta_n^2)+a_2\gamma_n^2-\omega^2] \exp[i(\alpha_n x+\beta_n y+\gamma_n z-\omega t)] \tag{16}$$

$$\Gamma \simeq \frac{1}{2\pi r} \sum_{n=1}^{N} \frac{-A_n \, i \, F_o \, \alpha_n \, \gamma_n^2 \, a_3}{|\underline{\nabla H}|\,(|K_H|)^{1/2}} \exp[i(\alpha_n x+\beta_n y+\gamma_n z-\omega t)] \tag{17}$$

where the symbol | | denote "the magnitude of". Now α, β and γ are the wave number components defining the singularities of the integrands in the integration process for which the residues are calculated. Eqn. (15) represents the residue corresponding to a single singularity point. For the eqns. (16) and (17) the wave number components are followed by the index n indicating that it is possible to have more than one singularity point and in this case the expressions for Δ and Γ represent the sum of the residues corresponding to each of the singularity points. N is the total number of singularity points over which the summation must be performed. Also

$$G = a_4(\alpha^2 + \beta^2) + a_5\gamma^2 - \omega^2 \tag{18}$$

$$|\underline{\nabla G}| = [G_{,\alpha}^2 + G_{,\beta}^2 + G_{,\gamma}^2]^{1/2} \tag{19}$$

$$H = [a_5\gamma^2+a_1(\alpha^2+\beta^2)-\omega^2][a_5(\alpha^2+\beta^2)+a_2\gamma^2-\omega^2]-a_3^2\gamma^2(\alpha^2+\beta^2) \tag{20}$$

$$|\underline{\nabla H}| = [H_{,\alpha}^2 + H_{,\beta}^2 + H_{,\gamma}^2]^{1/2} \tag{21}$$

$$K_G = \frac{G_{,\beta\beta}[G_{,\alpha}^2 C_{,\gamma\gamma} - 2G_{,\alpha} G_{,\gamma} C_{,\alpha\gamma} + G_{,\gamma}^2 G_{,\alpha\alpha}]}{(G_{,\alpha}^2 + G_{,\gamma}^2)^2} \tag{22}$$

$$K_H = \frac{H_{,\beta\beta}[H_{,\alpha}^2 H_{,\gamma\gamma} - 2H_{,\alpha} H_{,\gamma} H_{,\alpha\gamma} + H_{,\gamma}^2 H_{,\alpha\alpha}]}{(H_{,\alpha}^2 + H_{,\gamma}^2)^2} \tag{23}$$

$$r^2 = x^2 + y^2 + z^2 \tag{24}$$

The values K_G and K_H are commonly known as gaussian curvatures [1], and the combination of $|\underline{\nabla H}|$ and $(|K_H|)^{1/2}$ after simplification [2] is usually expressed by

$$\lambda_n = \frac{1}{|\underline{\nabla H}|(|K_H|)^{1/2}} = \left[\frac{H_{,\alpha}^2 + H_{,\gamma}^2}{H_{,\beta\beta}(H_{,\alpha}^2 H_{,\gamma\gamma} - 2H_{,\alpha} H_{,\gamma} H_{,\alpha\gamma} + H_{,\gamma}^2 H_{,\alpha\alpha})}\right]^{1/2} \tag{25}$$

A_n is a phase coefficient that is determined by the geometric properties of the H = 0 surface as follows:

a) $A_n = +1$ if $K_H > 0$ and $\underline{\nabla H}$ is in the +r direction;

b) $A_n = -1$ if $K_H > 0$ and $\underline{\nabla H}$ is in the -r direction;

c) $A_n = +1$ if $K_H < 0$ and $H = 0$ is convex in the $\underline{\nabla H}$ direction; and

d) $A_n = -1$ if $K_H < 0$ and $H = 0$ is concave in the $\underline{\nabla H}$ direction.

The values for A_n can be determined only by numerical calculations.

As mentioned before, eqns. (15), (16) and (17) are residues or sums of residues resulting from the integration process. In wave number space, $G = 0$ and $H = 0$ are surfaces containing all possible values of wave numbers that are able to generate such residues, considering the elastic properties of the material. Each point (α, β, γ) on the surfaces can then be associated with a particular wave train in a particular direction which effectively contributes to the displacement functions. It is important to observe that the $H = 0$ surface is in reality a quartic of two sheets [2]; so $H = 0$ defines two surfaces.

According to the method of stationary phase, the displacements at a point P in the medium are calculated by summing the contributions of plane waves passing through such a point [1]. These waves and the corresponding wave numbers can be found by locating the point (α, β, γ) or points $(\alpha_n, \beta_n, \gamma_n)$ on the surfaces $G = 0$ and $H = 0$, respectively, where the normal is parallel to the direction OP (in Fig. 1), which corresponds to finding the singularity points that generate the residues for the specific point P.

Note that normals to the G = 0 or H = 0 surfaces at more than one point may lie in the same direction (parallel to OP). In such a direction waves of different settings (direction of wave number vector) and spacings (magnitude of wave number vector) can be superposed and for this reason the summation signs appear in eqns. (16) and (17). It must be noted that this remark does not apply if the points are simply symmetric such as (α, β, γ) and $(-\alpha, -\beta, -\gamma)$ which correspond to waves of the same setting and spacing. For the solution satisfying the radiation condition, only one out of each such pair of points is selected. Geometrically, the surface G = 0 for a transversely isotropic medium is an ellipsoid and as a consequence there is only one point on the surface where the normal is parallel to OP.

With the use of eqns. (18) through (25), the expressions given in eqns. (15), (16) and (17) for the displacement functions can be rewritten as

$$\Lambda \tilde{=} \frac{\beta\, F_o [a_4^2(\alpha^2 + \beta^2) + a_5^2\, \gamma^2]}{4\pi r\, \omega\, (a_5\, Q)^{1/2}\, a_4} \exp\,[i(\alpha x + \beta y + \gamma z - \omega t)] \tag{26}$$

$$\Delta \tilde{=} \frac{1}{2\pi r} \sum_{n=1}^{N} A_n\, i\, \lambda_n\, F_o\, \alpha_n [a_5(\alpha_n^2+\beta_n^2) + a_2\gamma_n^2 - \omega^2]$$

$$\exp\,[i(\alpha_n x + \beta_n y + \gamma_n z - \omega t)] \tag{27}$$

$$\Gamma \tilde{=} \frac{1}{2\pi r} \sum_{n=1}^{N} A_n \, i \, \lambda_n \, F_o \, \alpha_n \, \gamma_n^2 \exp[i(\alpha_n x + \beta_n y + \gamma_n z - \omega t)] \tag{28}$$

where

$$Q = a_4^2(\alpha^2 + \beta^2) + a_5^2 \gamma^2 \tag{29}$$

The displacements u, v and w can be determined by assuming forms compatible with eqns. (26), (27) and (28) such that eqns. (12) are satisfied. Since the displacement functions are of exponential form, identical exponential forms are chosen to represent the displacements as

$$u = k_1 \Lambda + k_2 \Delta + k_3 \tag{30}$$

$$v = k_4 \Lambda + k_5 \Delta + k_6 \tag{31}$$

$$w = k_7 \Gamma + k_8 \tag{32}$$

where k_1 through k_8 are constants to be determined. If the derivatives of eqns. (30), (31) and (32) are calculated and terms involving the factor $1/r^2$ are neglected, the substitution of the resulting expressions for the derivatives into eqns. (12) gives the values of these constants as

$$k_1 = \frac{-\beta}{i(\beta^2 + \alpha^2)} \qquad k_2 = \frac{\alpha_n}{i(\alpha_n^2 + \beta_n^2)} \tag{33}$$

$$k_4 = \frac{\alpha}{i(\beta^2 + \alpha^2)} \qquad k_5 = \frac{\beta_n}{i(\alpha_n^2 + \beta_n^2)} \tag{34}$$

$$k_7 = \frac{1}{i\,\gamma_n}$$

The constants k_3, k_6 and k_8 are determined using the radiation condition presented earlier. Since there are no sources in the medium except at the origin, the displacements at infinity must vanish. This is possible only if the constants k_3, k_6 and k_8 are zero; so

$$k_3 = k_6 = k_8 = 0 \tag{36}$$

Therefore the final expressions for the displacements are

$$u \simeq \frac{\beta^2 F_o [a_4^2(\alpha^2 + \beta^2) + a_5^2\gamma^2]}{(\beta^2 + \alpha^2)\, 4\pi r\, \omega\, (a_5 Q)^{1/2} a_4} \exp[i(\alpha x + \beta y + \gamma z - \omega t)]$$

$$+ \frac{1}{2\pi r} \sum_{n=1}^{N} \frac{\alpha_n^2}{(\alpha_n^2+\beta_n^2)} A_n \lambda_n F_o [a_5(\alpha_n^2+\beta_n^2)+a_2\gamma_n^2-\omega^2]$$

$$\exp[i(\alpha_n x + \beta_n y + \gamma_n z - \omega t)] \tag{37}$$

$$v \cong - \frac{\alpha\beta\ F_o[a_4^2(\alpha^2+\beta^2) + a_5^2\gamma^2]}{(\alpha^2+\beta^2)4\pi r\ \omega(a_5 Q)^{1/2} a_4} \exp[i(\alpha x + \beta y + \gamma_z - \omega t)]$$

$$+ \frac{1}{2\pi r} \sum_{n=1}^{N} \frac{\alpha_n \beta_n}{(\alpha_n^2+\beta_n^2)} A_n\ \lambda_n\ F_o[a_5(\alpha_n^2+\beta_n^2) + a_2\ \gamma_n^2 - \omega^2]$$

$$\exp\ [i(\alpha_n x + \beta_n y + \gamma_n z - \omega t)] \tag{38}$$

$$w \cong - \frac{1}{2\pi r} \sum_{n=1}^{N} A_n\ \lambda_n\ F_o\ \alpha_n\ \gamma_n\ a_3 \exp\ [i(\alpha_n x + \beta_n y + \gamma_n z - \omega t)] \tag{39}$$

Observe that a different procedure could have been followed to obtain the expressions for the displacements. Recall that the expressions in eqns. (12) relate the displacements u, v and w with the displacement functions Λ, Γ and Δ. Then, from the expressions in eqns. (26), (27) and (28), the system represented by eqn. (12) could have been solved by direct integration. This procedure is mathematically more complex than the method of assuming exponential forms for u, v and w and determining constants as was done here.

PHASE VELOCITY AND WAVE SURFACE

In order to understand the propagation behavior of waves in anisotropic media, some concepts concerning the plane wave propagation characteristics are reviewed below. For this, consider the general equation of motion for an anisotropic medium when no body forces are present. From eqn. (8) with $F_j = 0$

$$C_{ijpq} u_{p,qi} - \rho u_{j,tt} = 0 \tag{40}$$

Assume a plane wave front of the form [5]

$$\phi = \phi[\underline{n}_r \cdot \underline{x} - |\underline{c}|^2 t] \tag{41}$$

where ϕ represents a characteristic with unit normal $\underline{n}_r$ and scalar phase velocity $|\underline{c}|$ along the normal direction. Observe that the characteristics represent the wave front in time and space. By the theory of characteristics, the displacements are functions of ϕ such that the spatial dependence of u is as $\underline{n}_r \cdot \underline{x}$.

For the nontrivial solution (that is, for the propagation of the front) the "characteristic condition" must be applied. This condition can be written as [5]

$$|C_{ijpq} \phi_{,i} \phi_{,q} - \rho \phi_{,t} \delta_{ip}| = 0 \tag{42}$$

or substituting the derivatives according eqn. (41) into eqn. (42) gives

$$|C_{ijpq}\, n_i\, n_q - \rho|\underline{c}|^2\, \delta_{ip}| = 0 \qquad (43)$$

where n_i and n_q are the projections (direction cosines) of $\underline{n}_r$ in the directions i and q, respectively, and δ_{ip} is the Kronecker delta.

The solution of eqn. (43) is an eigenvalue problem for the phase velocity $|\underline{c}|$ for any specified direction $\underline{n}_r$. In general, there are three velocities (that is, eigenvalues), distinct in magnitude for each $\underline{n}_r$.

Now suppose that the actual point source introduces the excitation into the medium. If composition of plane wave fronts is used to represent the actual disturbance front, according to Huygen's principle [5], the front can be traced out by the envelope of plane wave fronts as if they were generated at the origin in all possible directions, at time t = 0. So the normals $\underline{n}_r$ of the component plane fronts must assume all possible directions in order to sweep the entire space around the source. For each direction $\underline{n}_r$ a new determinant of the form shown in eqn. (42) is generated and three new eigenvelocities can be determined. Polar diagrams can be constructed for each of the three velocities as functions of the corresponding normal direction. The surfaces expressed in polar representation (diagrams) are called the velocity surfaces. Moreover, the envelope of plane wave fronts at unit time is called the wave surface [3]. There is a correspondence

between the velocity surface and the wave surface such that if three velocity surfaces exist, the same number of wave surfaces can be generated. The existence of three surfaces indicates that there are three possible modes of propagation, each mode with its particular phase velocities. If just one mode were to exist, the physical meaning of the wave surface could simply be stated as the boundary between the disturbed and undisturbed regions in the medium at unit time after the source is set into action.

Consider now the eigenvectors corresponding to the eigenvelocities. The symmetry of the forms in eqn. (42) indicates that the eigenvectors (that is, displacement modes) corresponding to each of the three eigenvalues are mutually orthogonal but in general none of them is parallel to the wave front normal direction $\underline{n}_r$ [2,5]. If one of the eigenvectors is coincident with the wave normal direction $\underline{n}_r$, the corresponding displacement mode is purely longitudinal and the above - mentioned orthogonality ensures that the remaining displacement modes are purely transverse. This condition is fulfilled for all wave propagation directions in isotropic media where each of the wave surfaces can be associated with a pure propagation mode, namely, one longitudinal mode and two transverse modes with perpendicular polarization planes.

For the transversely isotropic medium as opposed to the isotropic medium, the eigenvectors are not coincident with the wave normals in all directions, so plane wave fronts travel along directions oblique to their normal $\underline{n}_r$ [5]. This means that the modes of

propagation are combinations of longitudinal and transverse modes. Exceptions occur for certain directions. These directions are: (1) the principal direction perpendicular to the isotropic plane and (2) any direction contained in the isotropic plane. The values of the velocities for these directions, according to the convention adopted for the coordinate axes, are given in Table 1.

SLOWNESS SURFACE

The condition given in eqn. (43) for the existence of the solution of the equation of motion given in eqn. (40) can also be represented in terms of slownesses. The slowness $\underline{s}$ is generally defined as a vector whose magnitude is the inverse of the velocity magnitude $|\underline{c}|$, and whose direction is the same direction of $\underline{c}$, or

$$|\underline{s}| = 1/|\underline{c}| \tag{44}$$

For a system with three different velocities there are three such slowness vectors.

According to the form of the argument of the wave front function in eqn. (41) and the definition in eqn. (44), the component of $\underline{s}$ in the direction i, s_i, can be written as

$$s_i = n_i/|\underline{c}| \tag{45}$$

Substituting eqn. (45) into eqn. (43) gives

$$|C_{ijpq}\, s_i\, s_j - \rho\, \delta_{ip}| = 0 \tag{46}$$

The solution for the slownesses is the same as the solution for the velocities. As before, if each direction in space is considered, three surfaces can be traced out which are the reciprocals of the velocity surfaces [3]. The resulting surfaces are called slowness surfaces. Each radius vector from the origin to the surface on the slowness surface has its corresponding inverse on the velocity surface.

The slowness surface is then an alternative way of geometrically representing the propagation characteristics of materials. The solution for slowness is often preferred to the solution for velocities since the former involves simpler algebraic transformations. This argument is supported by the fact that the determinant from eqn. (43) leads to an expression of twelfth order in the velocities as opposed to the determinant from eqn. (46) which is a sixth order equation in s_i[5].

Recall, the case under study is that of a transversely isotropic medium subjected to an oscillatory point source. The motion is represented by eqns. (9), (10) and (11) in terms of the variables Λ, Γ, and Δ. The slowness surfaces can be identified when the differential equations (9), (10) and (11) are written in terms of their Fourier transforms [1], and the inverse transforms written for each variable Λ, Γ and Δ. In the inverse transform expressions, the expressions in α, β and γ defining the singularities of the integrand are automatically the slowness surfaces.

For the variable Λ, the associated slowness surface is the $G = 0$ surface where G is given in eqn. (18). This surface will be called SH. For the variables Γ and Δ, the remaining slowness surfaces are represented by $H = 0$ where H is given in eqn. (20). However, there are two surfaces that satisfy $H = 0$, resulting in two slowness surfaces [2,5]. These two surfaces will be called SV and P.

The physical meaning of the slowness surfaces SH, SV and P can be better pursued if the isotropic medium case is considered. For isotropic materials

$$a_1 = a_2,\ a_4 = a_5 \text{ and } a_3 = a_1 - a_5 \tag{47}$$

Further it can be shown that all three slowness surfaces are spherical. SV corresponds to purely rotational waves (purely transverse waves if plane waves are considered); SH corresponds to purely rotational waves (purely transverse waves if plane waves are considered); and P corresponds to purely dilatational waves (purely longitudinal waves if plane waves are considered). Moreover, the surfaces SH and SV are identical, meaning that shear waves with any polarization have exactly the same behavior in isotropic media.

Formally, the identification of the surfaces SV and SH can be accomplished by the corresponding intersections with coordinate axes as follows: SH is defined as the surface that contains the shear mode for plane waves in the x direction or the z direction with particle displacements in the y direction. SV is the surface that contains the shear mode for plane waves in the x and z directions with particle displacement in the z and x directions, respectively. Finally, the slowness surface P is defined as the surface that contains the longitudinal modes in the x and z directions. The correspondence between wave number components (α, β, γ) and geometric coordinates (x,y,z) is maintained here.

For transversely isotropic media the rotational and dilational propagation modes corresponding to the slowness surfaces are not pure, since in general the displacement vectors are not aligned

with the normals of the plane front segments that constitute the wave front. For wave propagation in the principal directions of the medium though, the waves can be purely rotational or purely dilatational. Specifically, the plane wave propagation along a principal direction, the rotational mode corresponds to a shear mode and the dilational mode corresponds to a longitudinal mode, just as for the isotropic medium. The identification of the surfaces SH, SV and P is done as explained above, by the intersections with the principal directions. An illustration of the slowness surfaces for a transversely isotropic medium is shown in Fig. 2. Observe that the values of the slownessess at the intersections of the surfaces with the coordinate axes are the inverses of the phase velocities presented in the previous section. The character of the corresponding plane waves along the principal directions is also sketched, showing the propagation and particle displacement directions.

GROUP VELOCITY

The group velocity $\underline{U}$ (or velocity of energy propagation) for the general anisotropic medium can be written according to Rayleigh's energy argument [13] extended to three dimensional propagation as [1]

$$\underline{U} = \frac{\nabla G}{-G,\omega} \tag{48}$$

where G is given by eqn. (18) and $\underline{U}$ has the direction of ∇G or, equivalently, the same direction as the normal to the slowness surface.

For points on the slowness surface G = 0, eqn. (48) can also be written as

$$\underline{U} = \frac{\omega \nabla G}{\underline{k} \cdot \nabla G} \tag{49}$$

where $\underline{k}$ is the wave number vector (α, β, γ). Observe that the correspondence between the wave number vector and the slowness vector is [1,3]

$$\underline{k} = \omega \underline{s} \tag{50}$$

such that $\underline{k}$ and $\underline{s}$ have the same orientation. The phase velocity in the $\underline{k}$ direction can be represented vectorially by

$$\underline{c} = \frac{\omega \underline{k}}{|\underline{k}|^2} \tag{51}$$

If eqns. (49) and (51) are compared, it can be seen that

$$\underline{U} \cdot \underline{k} = \underline{c} \cdot \underline{k} \tag{52}$$

Thus, the resultant of $\underline{U}$ in the $\underline{c}$ direction is $\underline{c}$, which is equivalent to saying that the velocity of energy propagation in the direction normal to the wave front is equal to the phase velocity.

Eqns. (48) through (52) are also valid for the two other slowness surfaces. The same results are obtained if G is replaced by H in the eqns. (48) through (52), provided that $\underline{k}$ is taken accordingly. Thus, there are three phase velocities and three group velocities for each direction in the medium.

Although eqn. (52) is satisfied, eqns. (49) and (51) indicate that $\underline{U}$ and $\underline{c}$ are different. There is a component of energy velocity in the direction parallel to the wave front, meaning that energy transmission is not in the same direction as wave motion. This is true for media where the phase speed varies with direction [1]. Thus, plane waves oblique to the principal directions can propagate along their own normals only if energy is also supplied in a direction parallel to the wave fronts.

APPLICATION EXAMPLE

Material Description

As an application example, a unidirectional composite material was chosen. The material was 3M Scotchply type 1002 fiberglass epoxy consisting of unidirectional E-glass in a 165° C curing epoxy matrix. The composite prepreg tape was cured in a heated press at $0.69\ 10^6\ N/m^2$. The resulting resin content was 36 percent by weight [18]. The properties of such composites depend not only on the volume fraction of the components but also on the fabrication method. Since knowledge of the elastic properties of the material was necessary for the numerical calculations, samples were fabricated for experiments. Ultrasonic methods [14,15,16,17] were used for the experimental measurements, relating wave speeds and elastic constants c_{ij}. The wave speeds were determined in the through - transmission configuration using tone bursts to generate either longitudinal or shear waves. The tests were performed at frequencies from 0.5 to 2.25 MHz in increments of 0.25 MHz.

The test specimens were cut in the form of rectangular prisms with uniform square cross sections from a 25.4 mm thick composite plate. The cross-sectional area was square with 12.7 mm sides. The lengths of the specimens ranged from 2.54 mm to 25.4 mm. The test specimen axes were oriented at various angles with respect to the fiber direction. The elastic constants were determined

from the measured longitudinal and shear wave speeds. The experimental values for the elastic constants are given in Table 2.

The convention adopted for the transversely isotropic medium in Fig. 1 was maintained here, so the z axis corresponded to the fiber direction. The density was 1850 kg/m^3 according to the manufacturer's data [18].

Slowness Surfaces

The slowness surfaces for the fiberglass epoxy material were calculated from G = 0 and H = 0, where G and H are given in eqns. (18) and (20) respectively. The forms of these equations indicate that both the surfaces are symmetric about γ for a rectangular coordinate system α, β, and γ. Thus, in order to determine the surfaces, only their intersections with the α-γ plane need to be calculated. Then, the entire slowness surfaces can be generated by revolving the intersection curves around the γ axis. Additionally, the intersection curves of the slowness surfaces G = 0 and H = 0 with the α-γ plane are symmetric with respect to α axis, which can be checked by setting β = 0 in eqns. (18) and (20). By the combination of all symmetries, only 1/4 of the intersections of the surfaces on the α-γ plane need to be calculated. The positive quadrant was chosen for the calculation.

The ranges of the variables are limited by the values shown in Fig. 2 which can be obtained by setting β = 0 and alternately, one at a time, α = 0 or γ = 0 in eqns. (18) and (20). For the positive quadrant the limits are:

For slowness surface SH: $0 \leq \frac{\alpha}{\omega} \leq 1/(a_4)^{1/2} \quad 0 \leq \frac{\gamma}{\omega} \leq 1/(a_5)^{1/2}$;

For slowness surface SV: $0 \leq \frac{\alpha}{\omega} \leq 1/(a_5)^{1/2} \quad 0 \leq \frac{\gamma}{\omega} \leq /(a_5)^{1/2}$; and

For slowness surface P: $0 \leq \frac{\alpha}{\omega} \leq 1/(a_1)^{1/2} \quad 0 \leq \frac{\gamma}{\omega} \leq 1/(a_2)^{1/2}$.

The surfaces are generated by the successive combination of the pairs (α,γ) satisfying eqn. (18) for SH and eqn. (20) for SV and P.

Fig. 3 shows the slowness surfaces SH, SV and P for the fiber-glass epoxy composite. In Fig. 3, points A and B are the so-called parabolic points on the slowness surface. At these points, the gaussian curvature based on eqn. (23) is zero. Geometrically, these are inflection points on the slowness surface. For the points of zero gaussian curvature, the amplitude coefficient λ_n(which corresponds to the inverse of a decay factor along the direction of the normal to the surface) goes to infinity which would give infinite displacement. The physical implications of the existence of such points can be better understood by analyzing the wave surfaces.

From the values obtained for slownesses, the velocity surfaces were calculated using eqn. (44) and are shown in Fig. 4. The velocity surfaces, namely V(SH), V(SV) and V(P) correspond, respectively, to the "inverses" of the slowness surfaces SH, SV and P.

Wave Surfaces

The wave surfaces can be directly obtained from the slowness surfaces. It can be shown [1] that the coordinates x, y and z of the wave surfaces can be calculated from $-G_{,\alpha}/G_{,\omega}$; $-G_{,\beta}/G_{,\omega}$; and $-G_{,\gamma}/G_{,\omega}$, respectively, for the wave surface corresponding to

the slowness surface SH, and by $-H_{,\alpha}/H_{,\omega}$;$-H_{,\beta}/H_{,\omega}$; and $-H_{,\gamma}/H_{,\omega}$ for the wave surfaces corresponding to the slowness surfaces SV and P. Fig. 5 shows the wave surfaces as calculated from the slowness surfaces SH, SV and P. The wave surface W (SH), which corresponds to SH, has the smallest phase velocities. The wave surface W(P), which corresponds to P, has the largest phase velocities.

As shown in Fig. 5, the wave surface corresponding to SV has two finite cuspidal edges [1,5]. The points at the tips of the cuspidal edges correspond to the inflection points A and B shown in Fig. 3. The directions defined by the lines from the origin to the tips of the cuspidal edges (Fig. 5) represent the directions for which the solution is not valid. These directions can be found to be at 41.970° and 62.545° with respect to the z axis. Since the wave fronts are geometrically similar in time, the cuspidal edges will be always located in the same direction with respect to the coordinate axes. Observe that for directions between the angles defined above, radii from the origin to the W(SV) wave surface may assume three distinct values as can be seen in Fig. 5, indicating that there are three contributions for the displacements of points in this region of space. The contributions arise because it is possible to find three points on the corresponding slowness surface where the normals have the same direction, according to the method of stationary phase. At a

point P in a direction in space between the angles 41.970° and 62.545, three plane wave fronts can be seen traveling along the direction OP from the origin (where the excitation is located). Thus, it is possible to have plane wave fronts of different orientations and different phase velocities passing through the same point in the medium at different times. In reality these plane wave fronts are segments that constitute the actual wave front.

Displacement Calculations

The displacements in a transversely isotropic medium subjected to a point force excitation as shown in Fig. 1 were also calculated for the fiberglass epoxy material.

A computer program was written that calculates the displacements at a given point P(x,y,z) in the material. The following steps were performed:

(1) Search for the point or points on each of the slowness surfaces in which the outward normals are parallel to the direction OP. This is done by comparing the direction defined by OP with the direction of the gradients to the slowness surfaces. The program retains the closest values to the direction given (one value for slowness surface SH; up to three values for slowness surface SV and up to two values for slowness surface P, in accordance with the possible number of points having the same normal direction). The wave numbers are determined from the coordinates of the selected points on the slowness surfaces via eqns. (18) and (20).

(2) Check the signs of the gaussian curvature and the direction of the gradient vector of the slowness surfaces, thus establishing the resulting phase coefficient A_n.

(3) Substitute into eqns. (36) through (38) the values found for α, β and γ and A_n above and calculate the contributions of each slowness surface to the displacements u, v and w.

Points in space were chosen and the corresponding displacements calculated. For simplicity the points were placed on the coordinate planes. The set of points chosen were:

(1) On the x-z plane, points along the arc $x^2 + z^2 = 4\ m^2$, and

(2) On the x-y plane, points along the arc $x^2 + y^2 = 4\ m^2$.

The frequency was set at 1 MHz and a load (body force) of unit amplitude (F_o = 1 N/kg) was applied. From eqns. (15), (16) and (17) it can be seen that if any of the gaussian curvatures is zero, the corresponding displacement function assumes an infinite value. It is known physically that no point in space may undergo an infinite displacement since the amplitude of excitation F_o is finite. It can be shown [2] mathematically that the discontinuities can be eliminated and the decay of the displacement amplitudes is found to vary as $r^{-5/6}$. In order to generate the amplitude coefficients, the points of discontinuity on the slowness surface SV are "avoided", which is equivalent to excluding the points A and B from the calculation set.

Figs. 6 through 9 show the polar diagrams of the displacement amplitudes for the points 2 m away from the origin on the x-y plane. Figs. 10 through 13 show the polar diagrams of the displacements amplitudes for the points 2 m away from the origin on the x-z plane. Observe that by reasons of loading symmetry, v displacements for points on the x-z plane are zero as well as w displacements for points on x-y plane. The curves are plotted separately according to the slowness surface that generates the contribution.

For points on the x-y plane, the contributions of the slowness surface SV are zero which implies that there are no shear waves

propagating along x direction with particle displacement in the z direction. Also, there are no shear waves propagating along the y direction with particle displacement in the z direction.

The contributions from the slowness surface P, Figs. 6 and 8, show that (1) there are pure longitudinal waves traveling along the x direction and this is the direction of maximum amplitude for u displacements (as expected since x is coincident with the force line); (2) no longitudinal waves travel in the y direction (zero amplitude component of v displacement for points in the y direction), and no shear waves with y polarization travel in the x direction (v displacements are zero in x direction).

The contributions from the slowness surface SH, Figs. 7 and 9, show that (1) there are pure shear waves in the y direction (with x polarization direction) but since v displacements along the y direction are zero, these are standing waves (y direction vibrates as a string); (2) no longitudinal waves travel in the y direction (zero amplitude component of v displacements for points in the y direction), and no shear waves with y polarization travel in the x direction (v displacements are zero in x direction).

For points on the x-z plane, the contributions of slowness surface SH are zero which implies that there are no shear waves propagating along the x direction with particle displacement in the y direction. Also there are no waves propagating along the z direction with particle motion in the y direction.

The contributions from the slowness surface SV, Figs. 10 and 11, show that (1) there are pure shear waves in the z direction (with x polarization direction) but since the w displacements along the z direction are zero these are standing waves (z direction vibrates as a string); (2) there are no shear waves traveling along the x direction (zero amplitude component of w displacement in the x direction).

The contributions from the slowness surface P, Figs. 11 and 13, show that (1) there are pure longitudinal waves propagating along the x direction and the u displacement amplitude along the x direction is larger than the corresponding u displacement amplitude along the z direction; (2) there are pure shear waves in the z direction (with x polarization direction) but since the w displacements along the z direction are zero these are standing waves.

By observing the polar diagrams of displacements (Figs. (6) through (13)), it can be seen that there are characteristic directions defining maxima for the displacement amplitudes. For comparison purposes these directions are listed in Table 3. It can be observed that there are two maxima for the contributions of slowness surface SV corresponding to the inflection points A and B in Fig. 3. For the contributions of the slowness surface P, the maxima occur at two other distinct positions. For the points on the plane x-y, the maxima occur along the line of force (x axis itself) for u displacements except for the small contribution of SH (see Fig. 7),

and at 45° for v displacements as expected, since x-y is isotropic. Slowness furfaces not listed in Table 3 have zero contributions to the corresponding displacements.

Recalling the relationship between strain energy and displacement amplitude (energy is proportional to the square of amplitude), it is clear that for points in regions of larger amplitudes the energy will assume the higher values. The difference between anisotropic and isotropic media is that the energy density for anisotropic media is not a uniform function for equal solid angles having vertexes at the origin, constructed around different directions in space. Lighthill [2] referred to this phenomenon saying that the energy is "confined" to some cone in space, or in other words, most of the energy travels along preferential directions. The preferential directions for the unidirectional fiberglass epoxy composite are shown in Table 3. It is understood that the maxima are the center directions of the regions around which the energy is confined. When the numerical process is carried out the preferential directions are automatically determined.

CONCLUSIONS

The far-field displacement pattern in an infinite transversely isotropic medium subjected to an oscillatory point force was determined and evaluated for a specific fiberglass epoxy composite. The solution describes the stress wave field in terms of the geometric aspects of the disturbance spreading by means of slowness and wave surfaces. The solution for displacements allows the prediction of the amplitude distribution as shown by the construction of polar diagrams.

It was seen that the energy from a point source travels along radial directions even if the wave surfaces assume complicated shapes, meaning that the phase and group velocities are different.

The existence of preferential directions is an important aspect to be considered when experimental tests are to be designed. Knowledge of the displacement field allows a better choice to be made for the positioning of components of the measuring system.

There appear to be no restrictions regarding the applicability of this method to other types of anisotropy. If appropriate symmetry relations can be applied as in the case of eqn. (7), the same procedures can be followed for the displacement field solution. This possibility is attractive for use in the description of the stress wave field of filamentary composite materials with fiber arrangements other than unidirectional.

Another possible application is the study of acoustic emission (AE) phenomena in composites or other anisotropic materials. It is known that acoustic emission is a transient disturbance of relatively small dimensions occurring inside the material, and normally

containing a range of frequency components. If the method is applied for each component of frequency, superposition can be used for the determination of the field resulting from the AE source. Knowledge of the displacement field might allow inferences regarding the source such as strength and orientation, and consequently perhaps the degree of damage within the material.

REFERENCES

[1] M.J. Lighthill, "Studies on Magneto-Hydrodynamic Waves and other Anisotropic Wave Motions", Philosophical Transactions of the Royal Society, Series A, Vol. 252, 1960, pp. 397-430.

[2] V.T. Buchwald, "Elastic Waves in Anisotropic Media", Proceedings of the Royal Society, Series A, Vol. 253, 1959, pp. 563-580.

[3] J.L. Synge, "Elastic Waves in Anisotropic Media", Journal of Mathematics and Physics, Vol. 25, 1956, pp. 323-334.

[4] G.F. Carrier, "The Propagation of Waves in Orthotropic Media", Quarterly of Applied Mathematics, Vol. 4, 1946, pp. 160-165.

[5] M.J.P. Musgrave, Crystal Acoustics; Introduction to the Study of Elastic Waves and Vibrations in Crystals, Holden Day, San Francisco, 1970.

[6] J.D. Achenbach, A Theory of Elasticity with Microstructure for Directionally Reinforced Composites, OISM-Courses and Lectures, No. 167 (International Center for Mechanical Sciences), Springer-Verlag, N.Y., 1965.

[7] J.E. White and F.A. Angona, "Elastic Waves in Laminated Media", The Journal of the Acoustical Society of America, Vol. 17, No. 2, 1955, pp. 310-317.

[8] B.W. Rosen, "Stiffness of Fibre Composite Materials", Composites, Vol. 4, No. 1, 1973, pp. 16-25.

[9] A.E.H. Love, A Treatice on the Mathematical Theory of Elasticity, Dover, 4th Edition, 1944.

[10] S.G. Lekhnistskii, Theory of Elasticity of an Anisotropic Elastic Body, Holden Day, San Francisco, 1963, (translation).

[11] I.S. Sokolnikoff, Mathematical Theory of Elasticity, McGraw Hill, NY, 1956.

[12] K.F. Graff, Wave Motion in Elastic Solids, Ohio State University Press, 1975.

[13] L. Rayleigh, Theory of Sound, Vol. 2, Dover, 1945.

[14] G.D. Dean and F.J. Lockett, "Determination of the Mechanical Properties of Fiber Composites by Ultrasonic Techniques", Analysis of the Test Methods for High Modulus Fibers and Composites, ASTM STP521, American Society for Testing Materials, 1973, pp. 326-345.

[15] G.D. Dean, "Characterization of Fibre Composites using Ultrasonics", Composites-Standards, Testing and Design, National Physics Laboratory Conference Proceedings, Middlesex, England, 1974, pp. 126-130.

[16] J.H. Williams, Jr., H.N. Hashemi and S.S. Lee, "Ultrasonic Attenuation and Velocity in AS/3501-6 Graphite/Epoxy Fiber Composite", Journal of Nondestructive Evaluation, Vol. 1, No. 2, 1980, pp. 137-148.

[17] M.F. Markham, "Measurements of the Elastic Constants of Fibre Composites by Ultrasonics", Composites, Vol. 1, No. 3, 1970, pp. 145-149.

[18] "Scotchply Reinforced Plastics Technical Data - Type 1002", 3M Company, Minnesota, May 1, 1969.

TABLE 1 Velocities for Plane Waves along Principal Directions of Transversely Isotropic Media. (x-y is isotropic plane)

Direction of Propagation	Direction of Displacement Vector x	y	z
x	$(a_1)^{1/2}$	$(a_4)^{1/2}$	$(a_5)^{1/2}$
y	$(a_4)^{1/2}$	$(a_1)^{1/2}$	$(a_5)^{1/2}$
z	$(a_5)^{1/2}$	$(a_5)^{1/2}$	$(a_2)^{1/2}$

The a_i are defined in eqn. (13).

TABLE 2 Elastic Constants for Unidirectional Fiberglass Epoxy Composite (Scotchply 1002).

Elastic Constant	Computed Value from Wave Speed Measurements
C_{11}	10.580 10^9 N/m^2
C_{12}	4.098 10^9 N/m^2
C_{13}	4.679 10^9 N/m^2
C_{33}	40.741 10^9 N/m^2
C_{44}	4.422 10^9 N/m^2

TABLE 3 Points of Maximum Displacement Amplitude for Lines on x-z Plane and x-y Plane

Line Equation	Displm	Slowness Surfaces	Maximum Location	Order of Magnitude of Amplitudes (***)
$x^2 + z^2 = 4$	u	SV	41°; 62.5° (*)	10^{-8}
		P	90° (*)	10^{-8}
	w	SV	42°; 62.6° (*)	10^{-9}
		P	15° (*)	10^{-9}
$x^2 + y^2 = 4$	u	SH	0° (**)	10^{-8}
		P	90° (**)	10^{-9}
	v	SH	45° (**)	10^{-9}
		P	45° (**)	10^{-9}

(*) Angles with respect to z axis (in degrees)

(**) Angles with respect to y axis (in degrees)

(***) These amplitudes correspond to a unit body force.

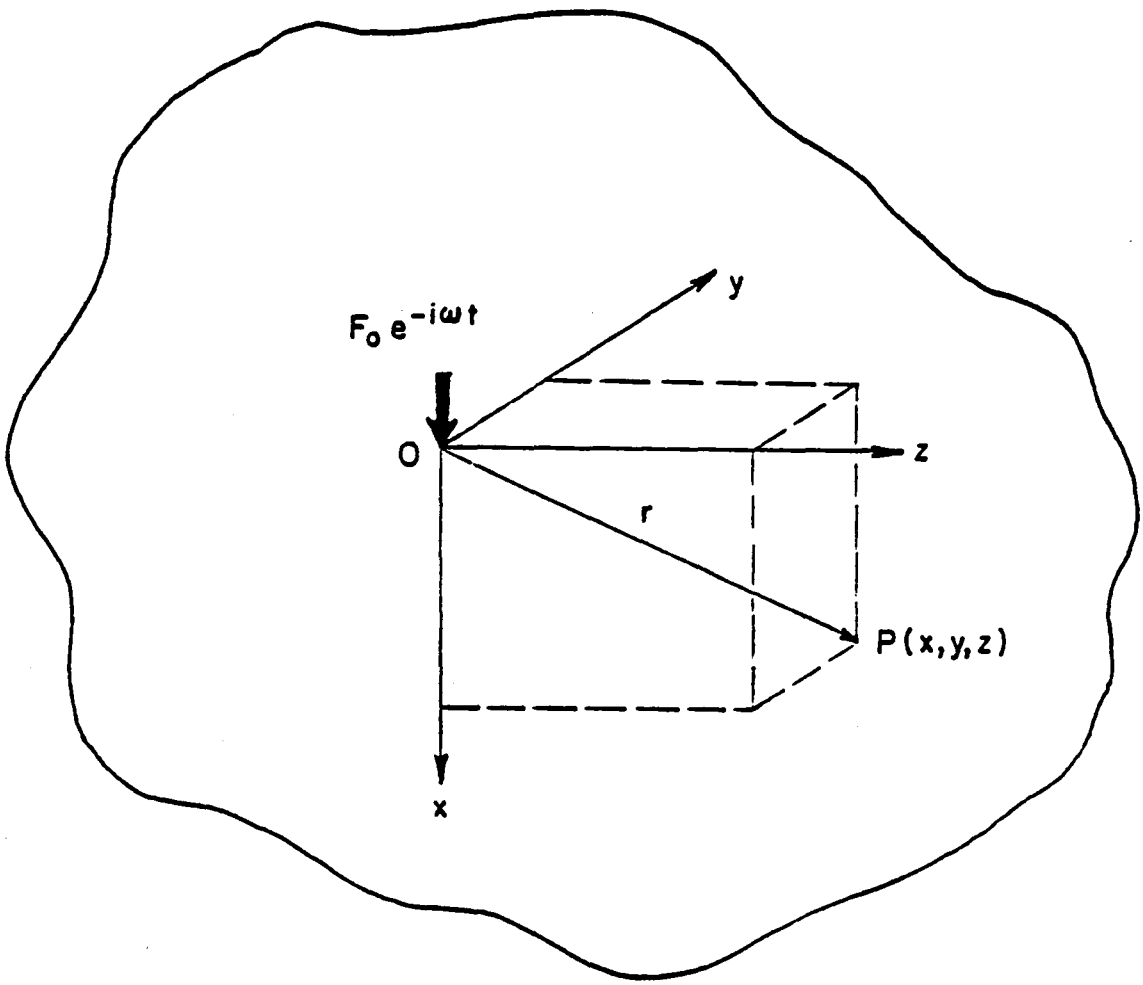

Fig. 1 Schematic illustrating sinusoidal point load exciting an infinite transversely isotropic medium, where xy is isotropic plane in cartesian coordinate system defined by (x,y,z).

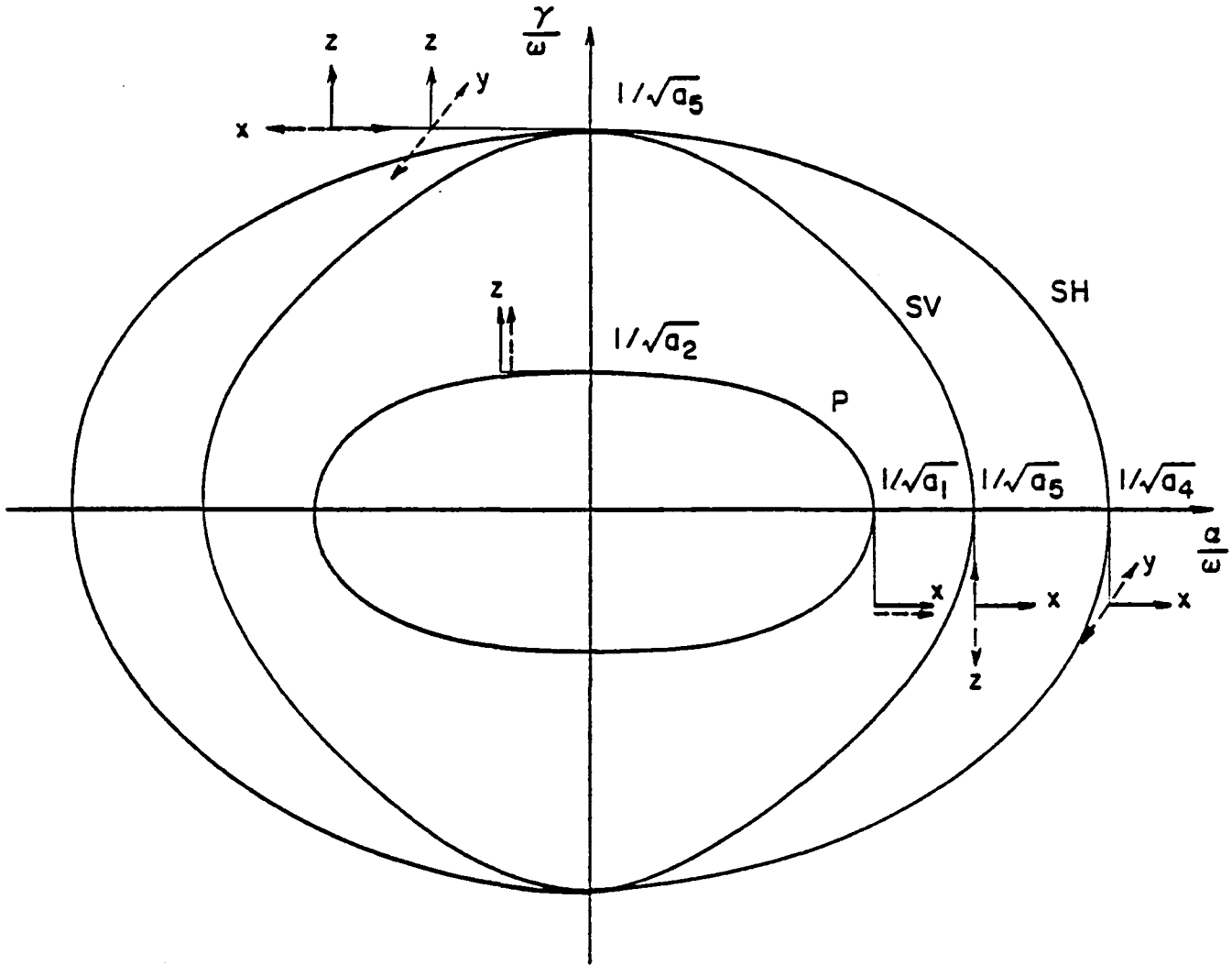

α – wave number vector component in x direction

γ – wave number vector component in z direction

⟶ Propagation direction of associated plane wave (along principal directions)

⇢ Particle displacement of associated plane wave (along principal directions)

Fig. 2 Plane representation of slowness surfaces for transversely isotropic medium where z axis corresponds to the larger elastic constant value and x-y is the isotropic plane.

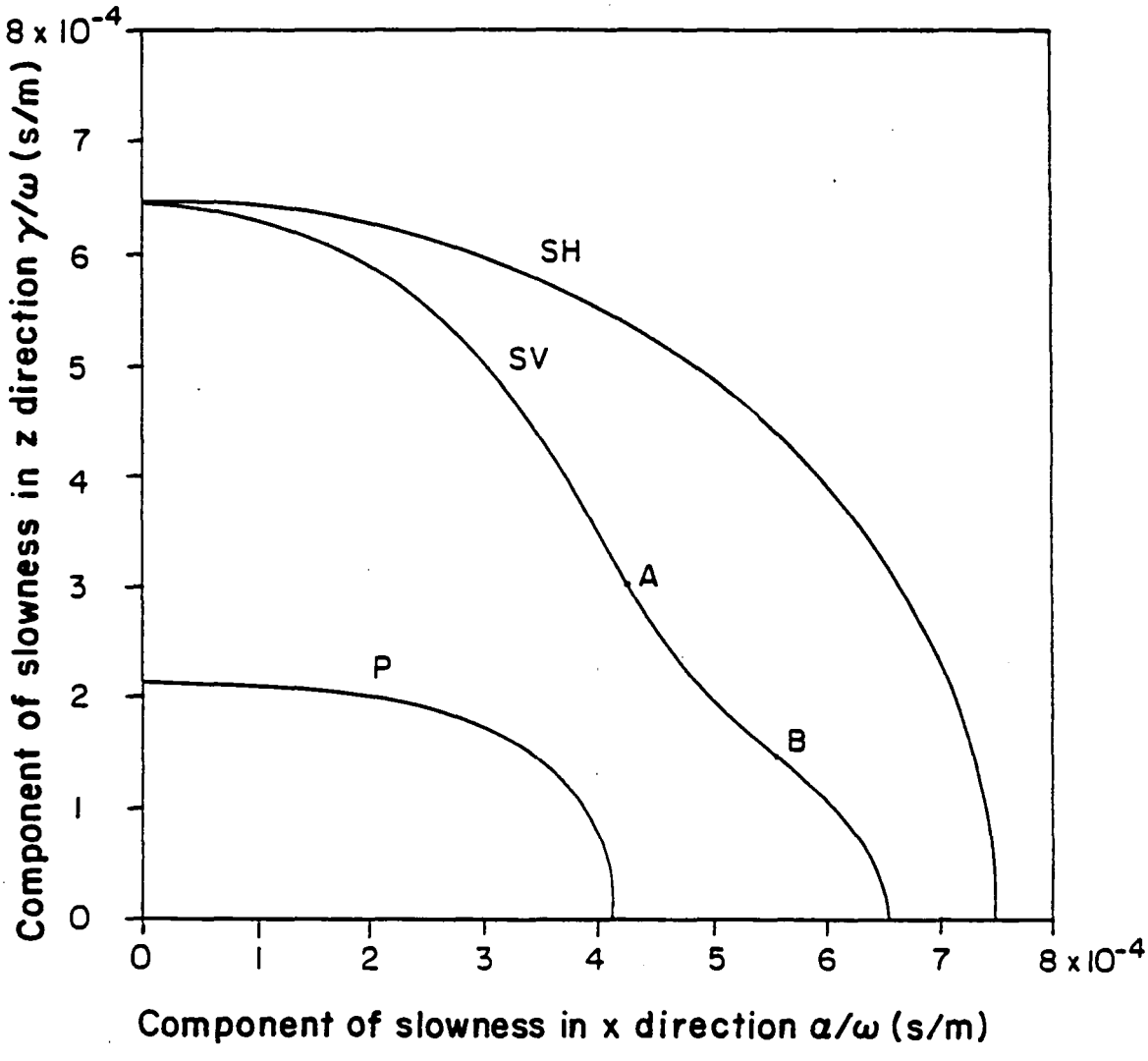

Fig. 3 Slowness surfaces SH, SV and P for unidirectional fiberglass composite for positive x-z quadrant.

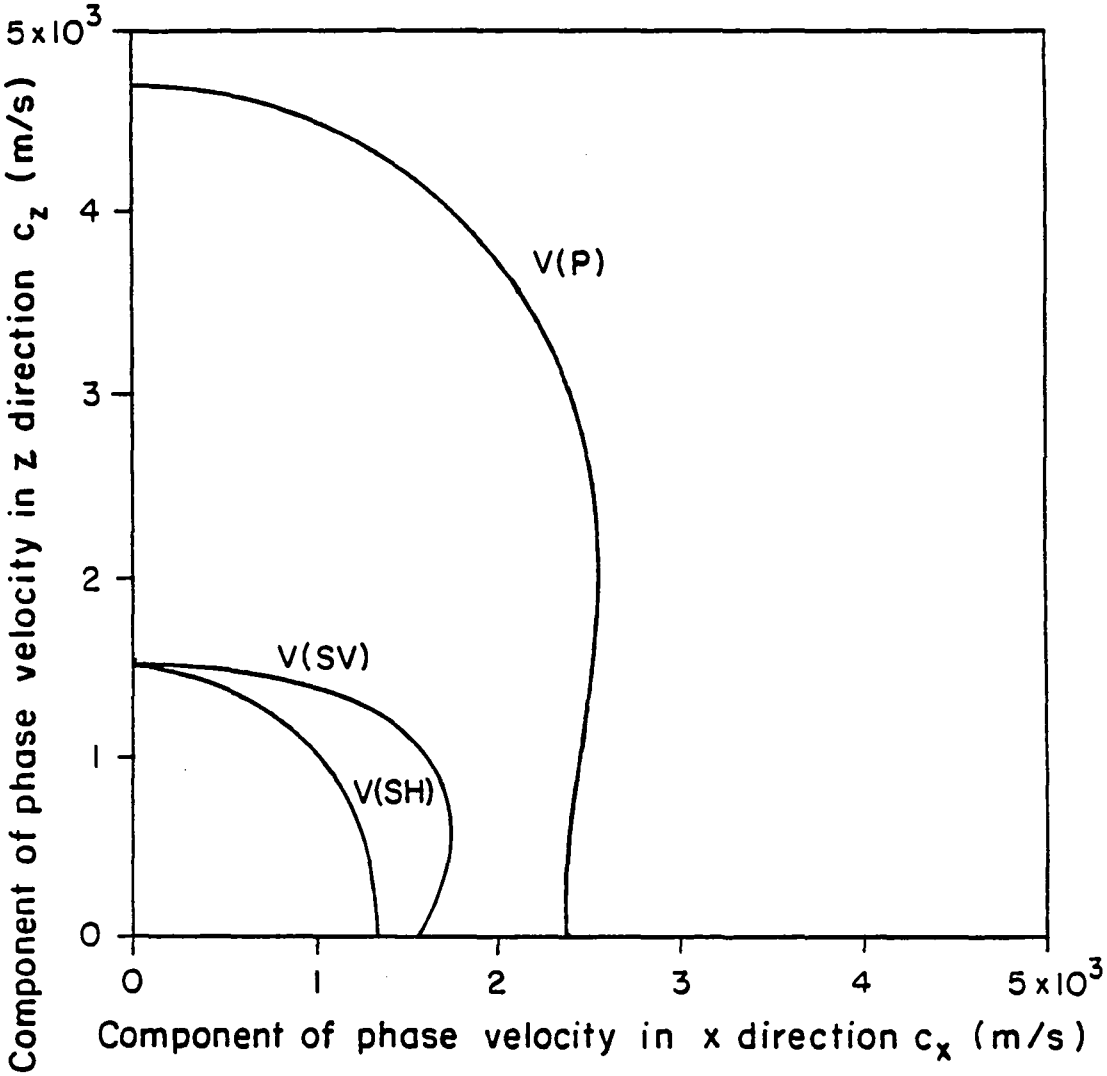

Fig. 4 Velocity surfaces V(SH), V(SV) and V(P) for unidirectional fiberglass composite for positive x-z quadrant.

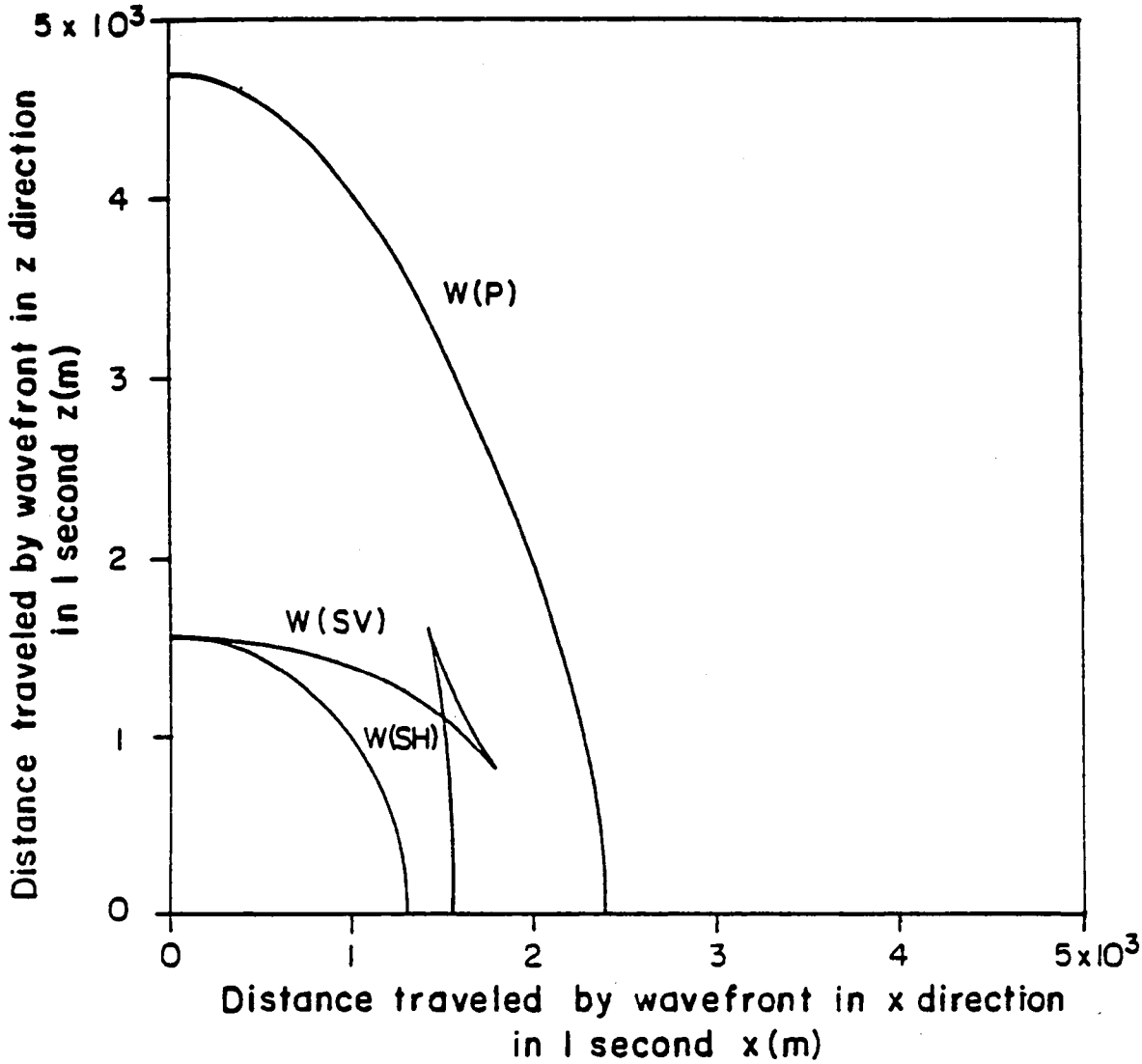

Fig. 5 Wave surfaces W(SH), W(SV) and W(P) for unidirectional fiberglass composite for positive x-z quadrant.

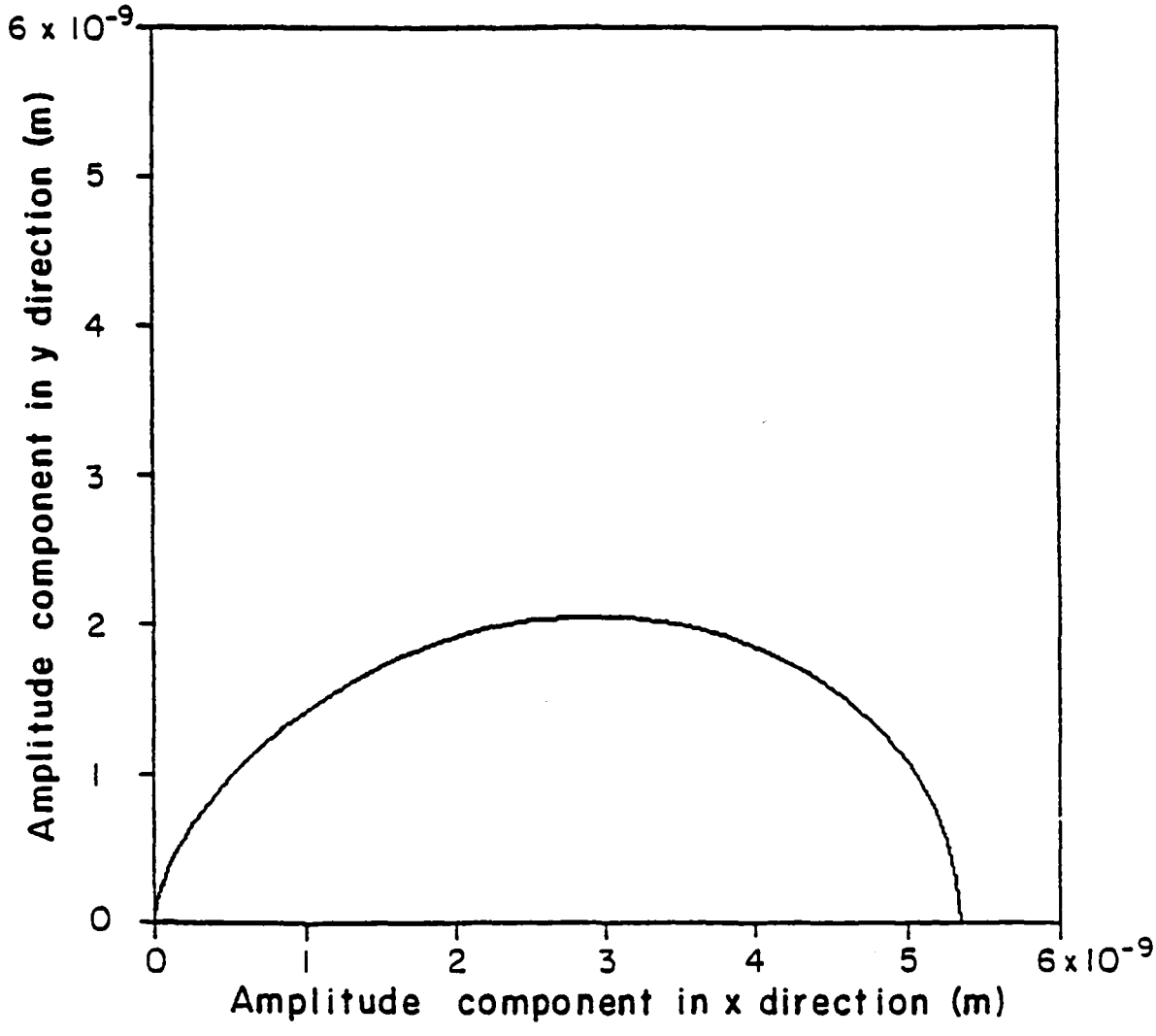

Fig. 6 Polar diagram for u displacement amplitudes for points along the line $x^2 + y^2 = 4m^2$, due to slowness surface P only.

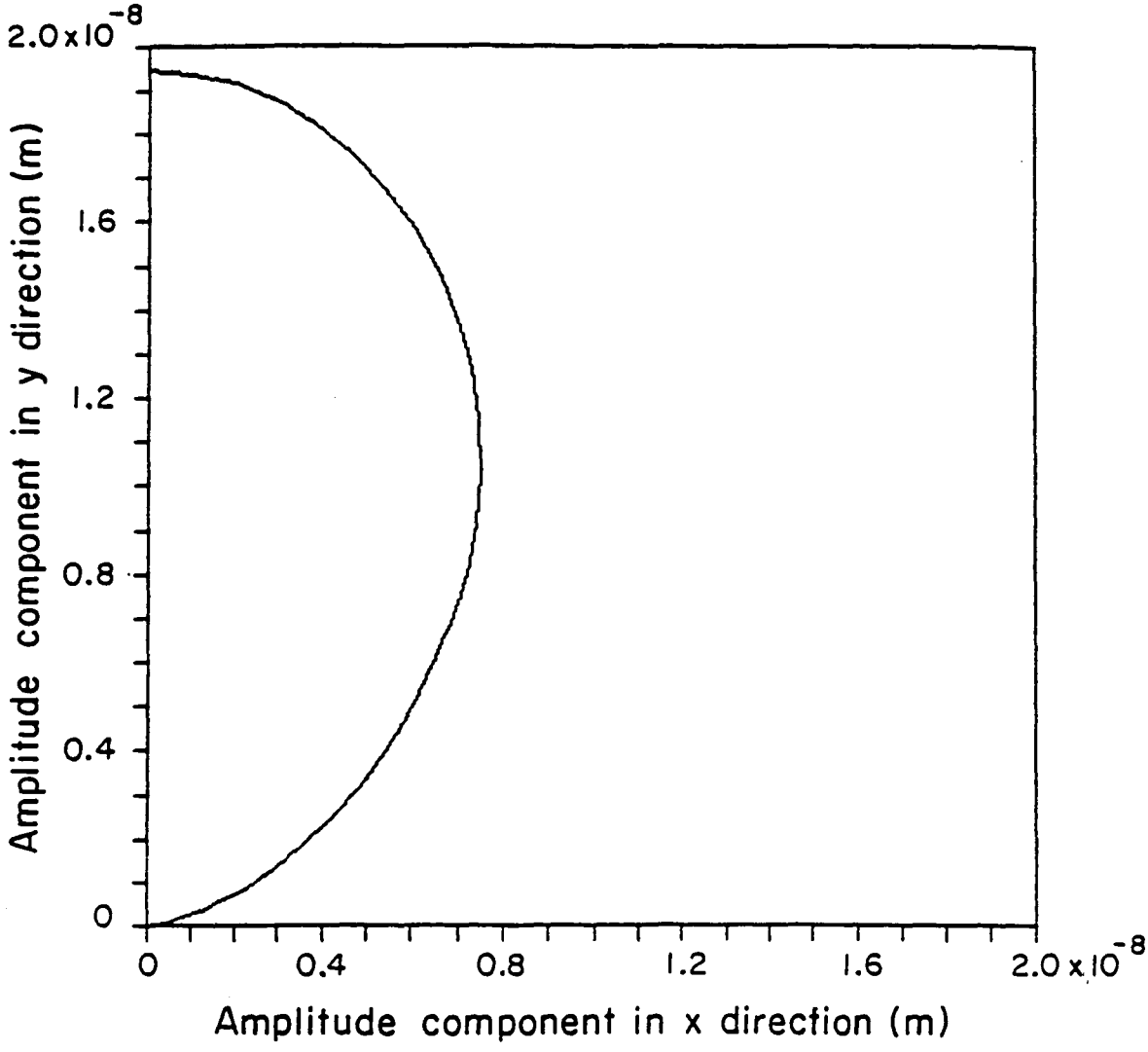

Fig. 7 Polar diagram for u displacement amplitudes for points along the line $x^2 + y^2 = 4m^2$, due to slowness surface SH only.

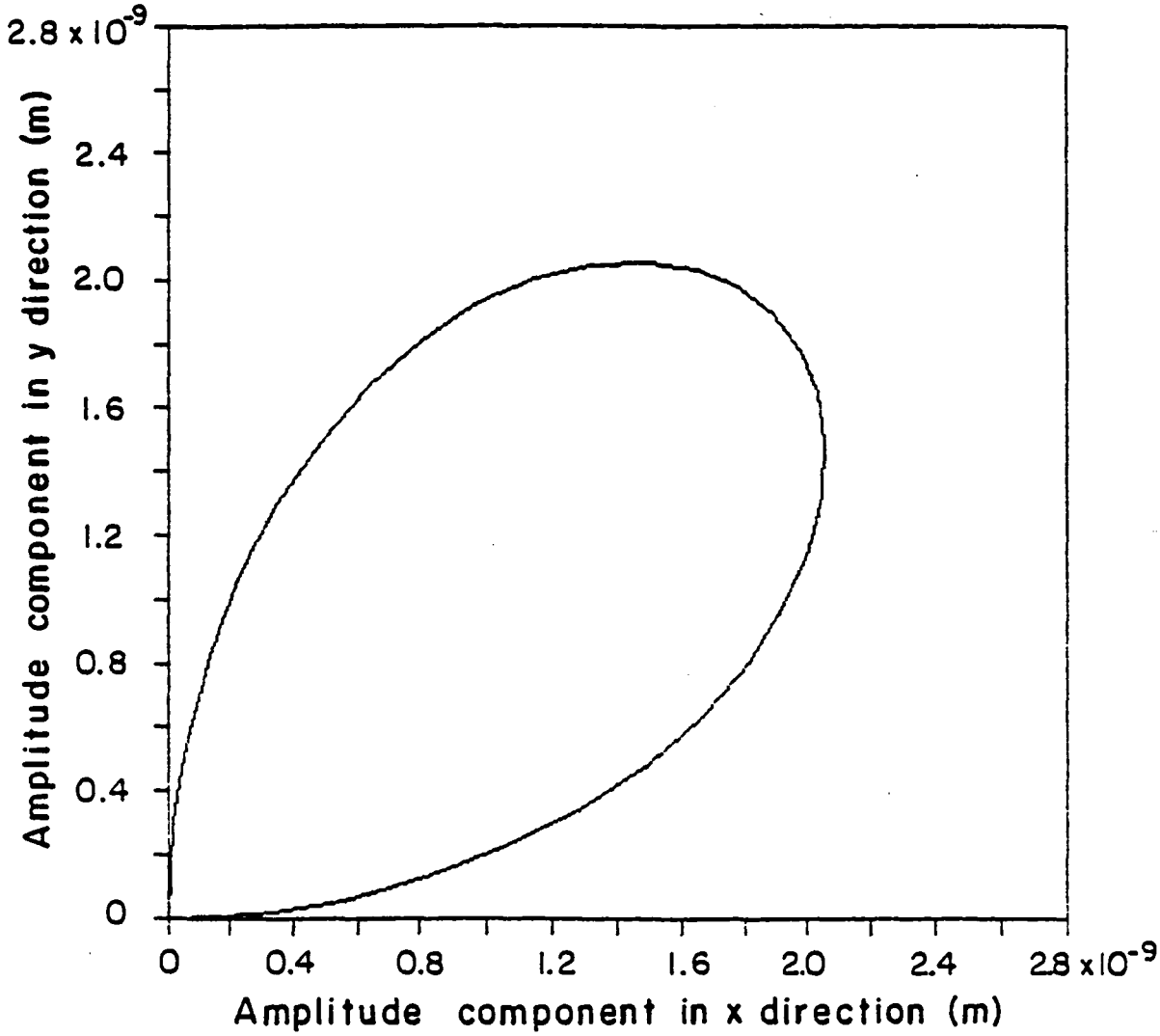

Fig. 8 Polar diagram for v displacement amplitudes for points along the line $x^2 + y^2 = 4m^2$, due to slowness surface P only.

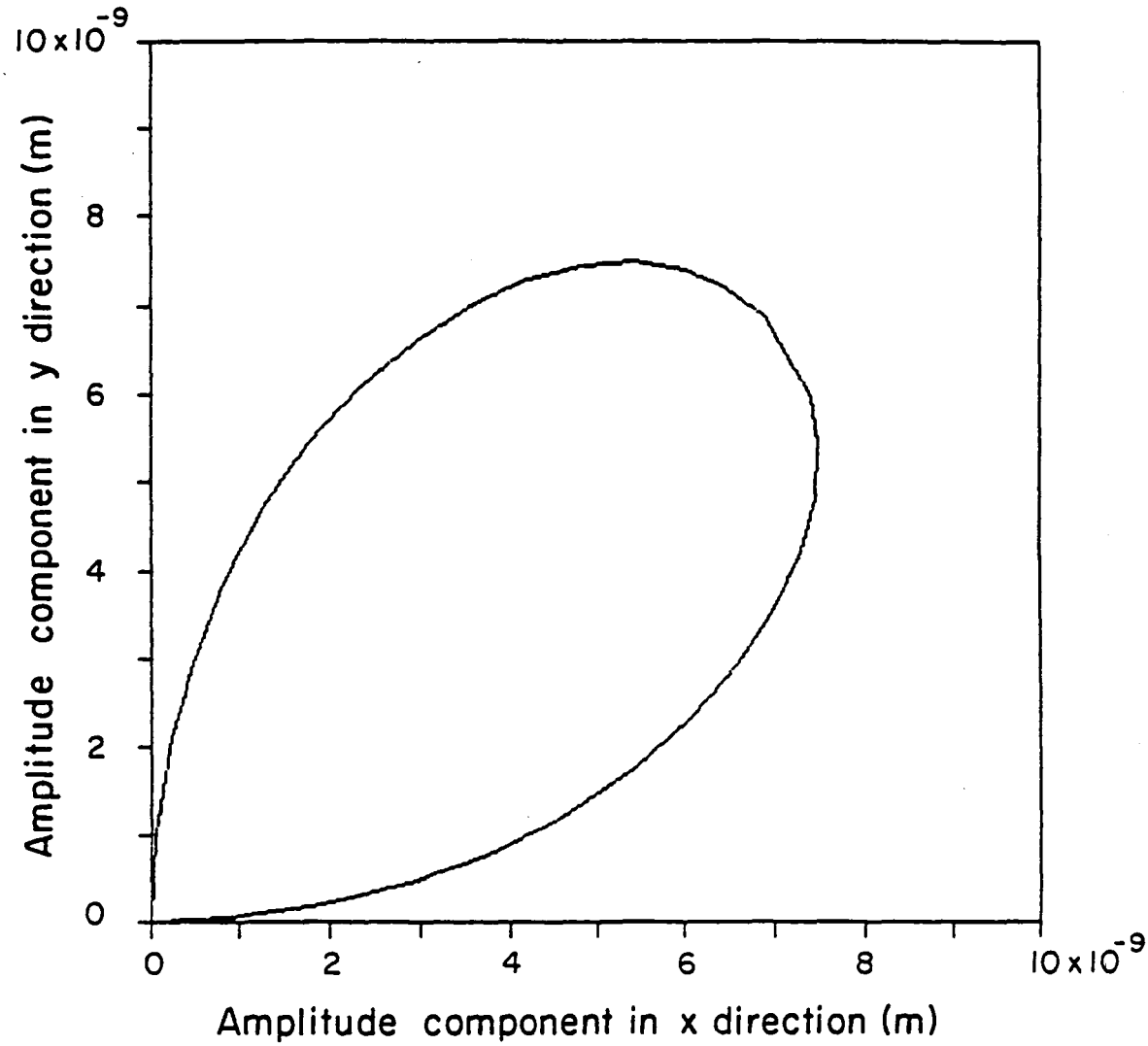

Fig. 9 Polar diagram for v displacement amplitudes for points along the line $x^2 + y^2 = 4m^2$, due to slowness surface SH only.

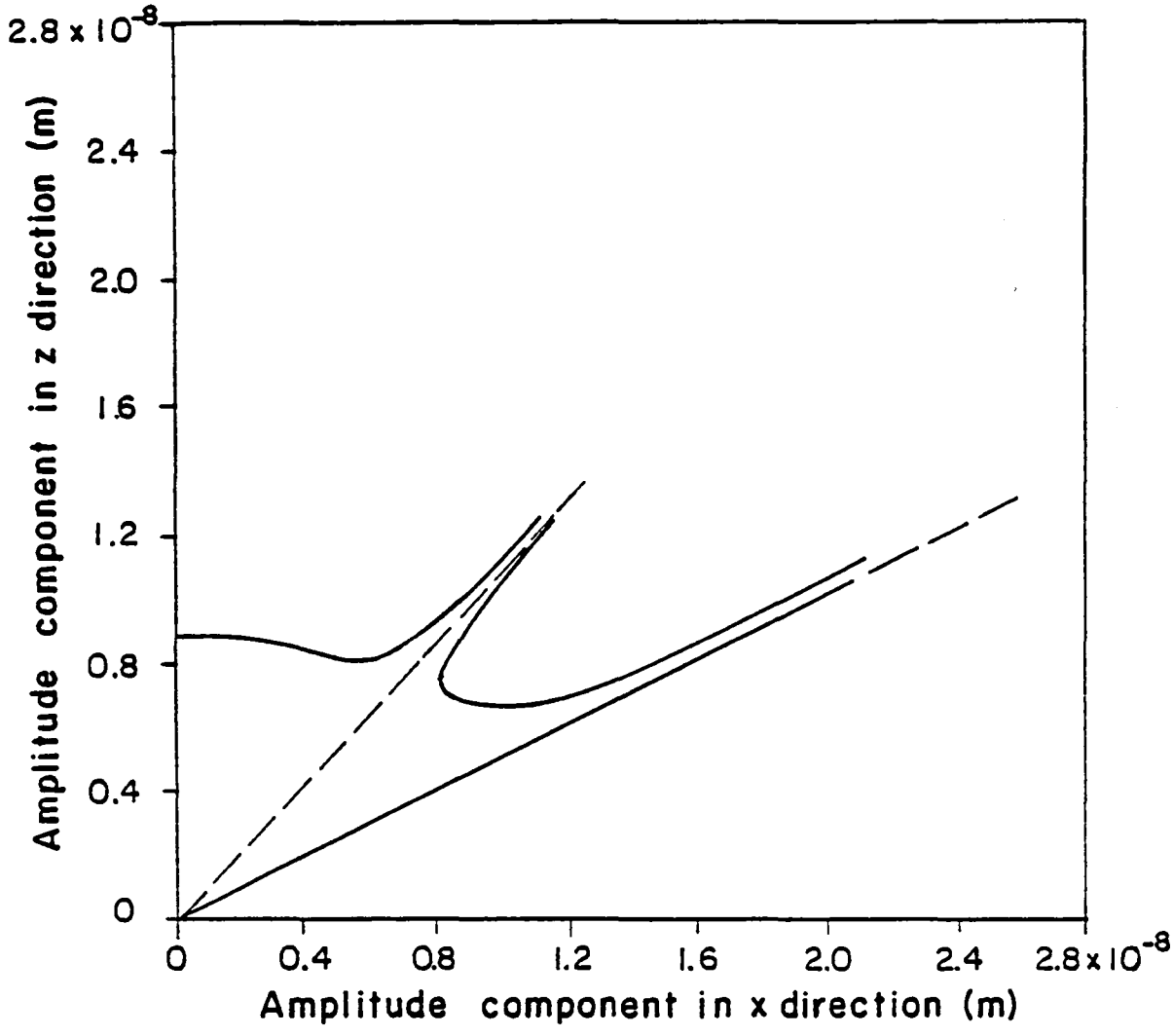

Fig. 10 Polar diagram for u displacement amplitudes for points along the line $x^2 + z^2 = 4m^2$, due to slowness surface SV only.

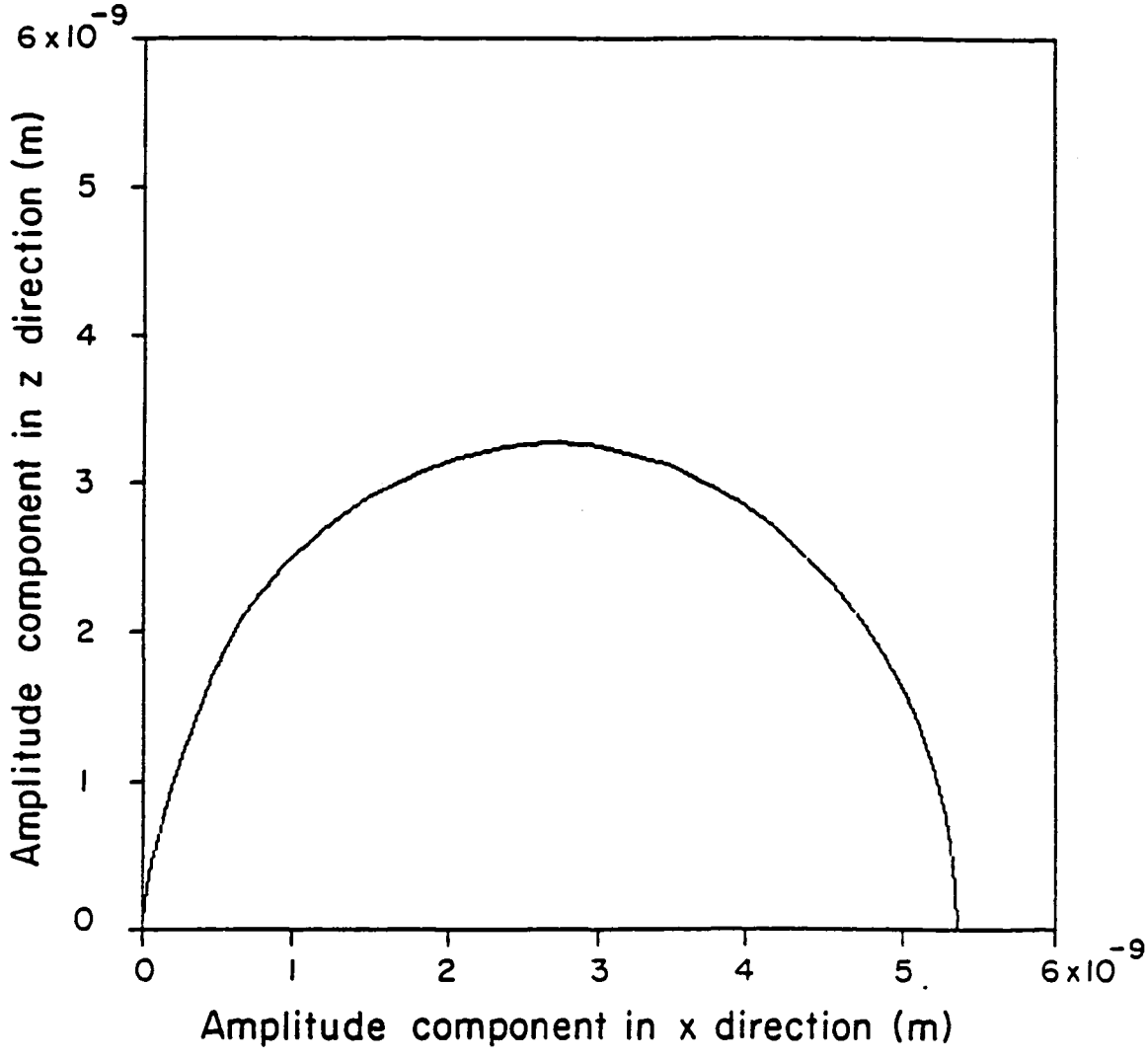

Fig. 11 Polar diagram for u displacement amplitudes for points along the line $x^2 + z^2 = 4m^2$, due to slowness surface P only.

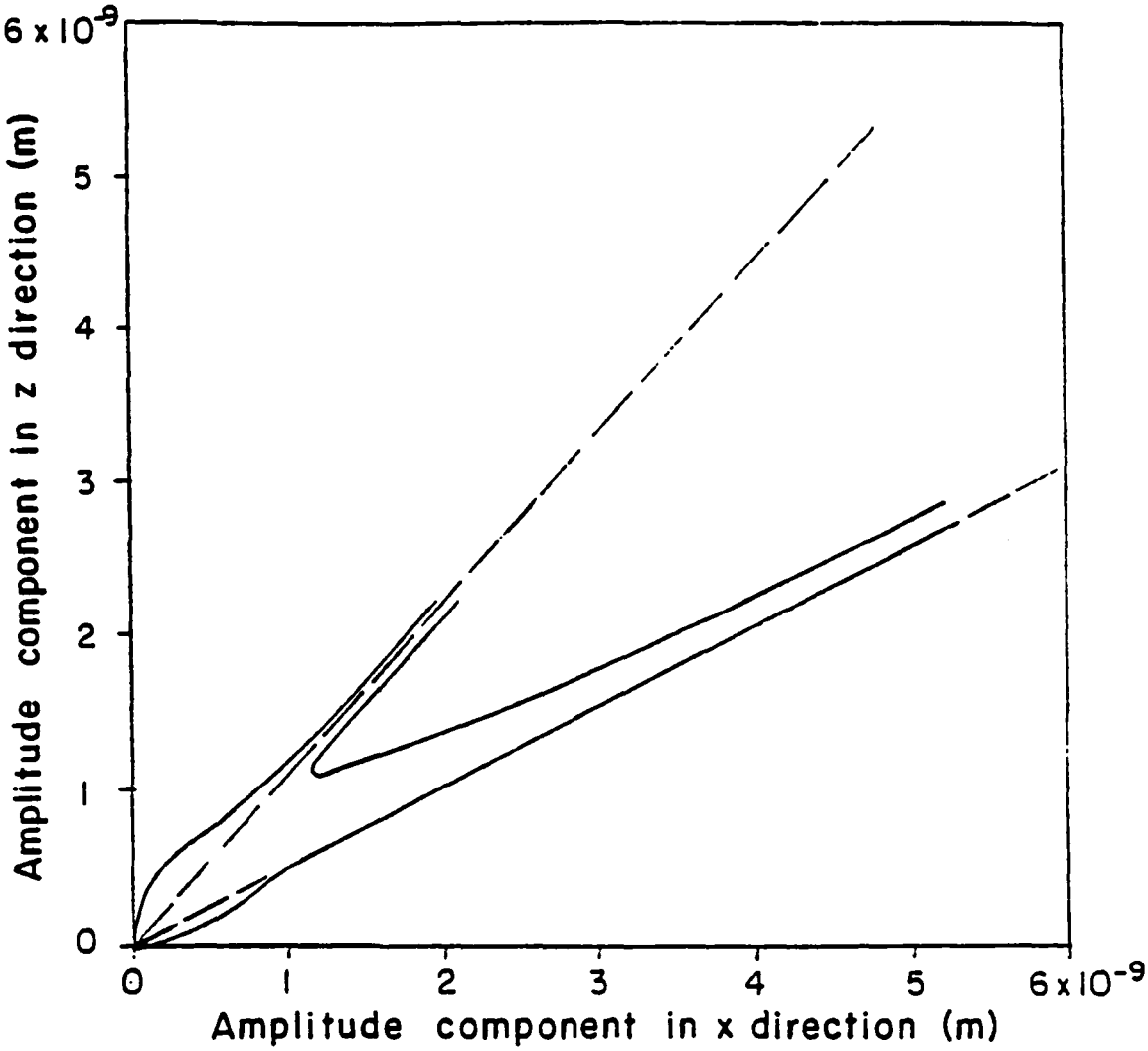

Fig. 12 Polar diagram for w displacement amplitudes for points along the line $x^2 + z^2 = 4m^2$, due to slowness surface SV only.

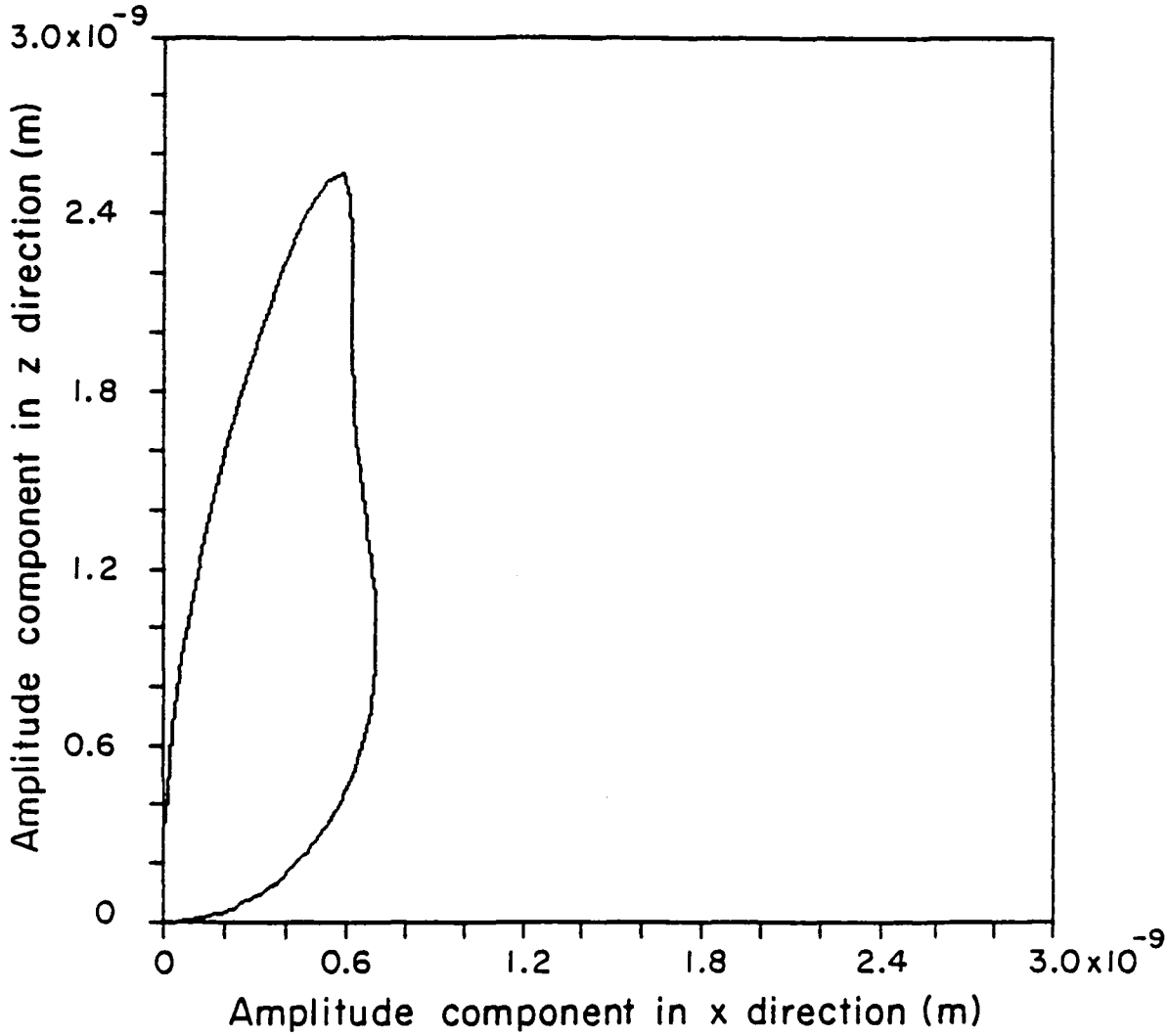

Fig. 13 Polar diagram for w displacement amplitudes for points along the line $x^2 + z^2 = 4m^2$, due to slowness surface P only.

1. Report No.	2. Government Accession No.	3. Recipient's Catalog No.
NASA CR-4001		

4. Title and Subtitle	5. Report Date
Wave Propagation in Anisotropic Medium Due to an Oscillatory Point Source With Application to Unidirectional Composites	July 1986
	6. Performing Organization Code

7. Author(s)	8. Performing Organization Report No.
James H. Williams, Jr., Elizabeth R. C. Marques, and Samson S. Lee	None
	10. Work Unit No.

9. Performing Organization Name and Address	11. Contract or Grant No.
Massachusetts Institute of Technology Department of Mechanical Engineering Cambridge, Massachusetts 02139	NAG3-328
	13. Type of Report and Period Covered
12. Sponsoring Agency Name and Address	Contractor Report
National Aeronautics and Space Administration Washington, D.C. 20546	14. Sponsoring Agency Code
	506-43-11 (E-3093)

15. Supplementary Notes

Final report. Project Manager, Alex Vary, Structures Division, NASA Lewis Research Center, Cleveland, Ohio 44135.

16. Abstract

The far-field displacements in an infinite transversely isotropic elastic medium subjected to an oscillatory concentrated force are derived. The concepts of velocity surface, slowness surface and wave surface are used to describe the geometry of the wave propagation process. It is shown that the decay of the wave amplitudes depends not only on the distance from the source (as in isotropic media) but also depends on the direction of the point of interest from the source. As an example, the displacement field is computed for a laboratory-fabricated unidirectional fiberglass epoxy composite. The solution for the displacements is expressed as an amplitude distribution and is presented in polar diagrams. This analysis has potential usefulness in the acoustic emission (AE) and ultrasonic nondestructive evaluation of composite materials. For example, the transient localized disturbances which are generally associated with AE sources can be modeled via this analysis. In which case, knowledge of the displacement field which arrives at a receiving transducer allows inferences regarding the strength and orientation of the source, and consequently perhaps the degree of damage within the composite.

17. Key Words (Suggested by Author(s))	18. Distribution Statement
Elastic waves; Ultrasonics; Acoustic emission; Wave propagation analysis; Nondestructive testing; Fiber reinforced composites	Unclassified - unlimited STAR Category 38

19. Security Classif. (of this report)	20. Security Classif. (of this page)	21. No. of pages	22. Price*
Unclassified	Unclassified	58	A04

*For sale by the National Technical Information Service, Springfield, Virginia 22161

NASA-Langley, 1986

End of Document